

# RElectrode: A Reconfigurable Electrode For Multi-Purpose Sensing Based on Microfluidics

Wei Sun<sup>1,2</sup>, Yanjun Chen<sup>1</sup>, Simon Zhan<sup>4</sup>, Teng Han<sup>1,3\*</sup>

Feng Tian<sup>1,3</sup>, Hongan Wang<sup>1</sup>, Xing-Dong Yang<sup>5</sup>

<sup>1</sup>State Key Laboratory of Computer Science and Beijing Key Lab of Human-Computer Interaction, Institute of Software, Chinese Academy of Sciences, Beijing, China

<sup>2</sup>School of Computer Science and Technology, University of Chinese Academy of Sciences, Beijing, China

<sup>3</sup>School of Artificial Intelligence, University of Chinese Academy of Sciences, Beijing, China

<sup>4</sup> University of California, Berkeley, California, United States

<sup>5</sup>Department of Computer Science, Dartmouth College, Hanover, New Hampshire

<sup>1</sup>{sunwei2017,chenyanjun, hanteng, tianfeng, hongan}@iscas.ac.cn, <sup>2</sup>simonzhan@berkeley.edu,  
<sup>3</sup>xing-dong.yang@dartmouth.edu

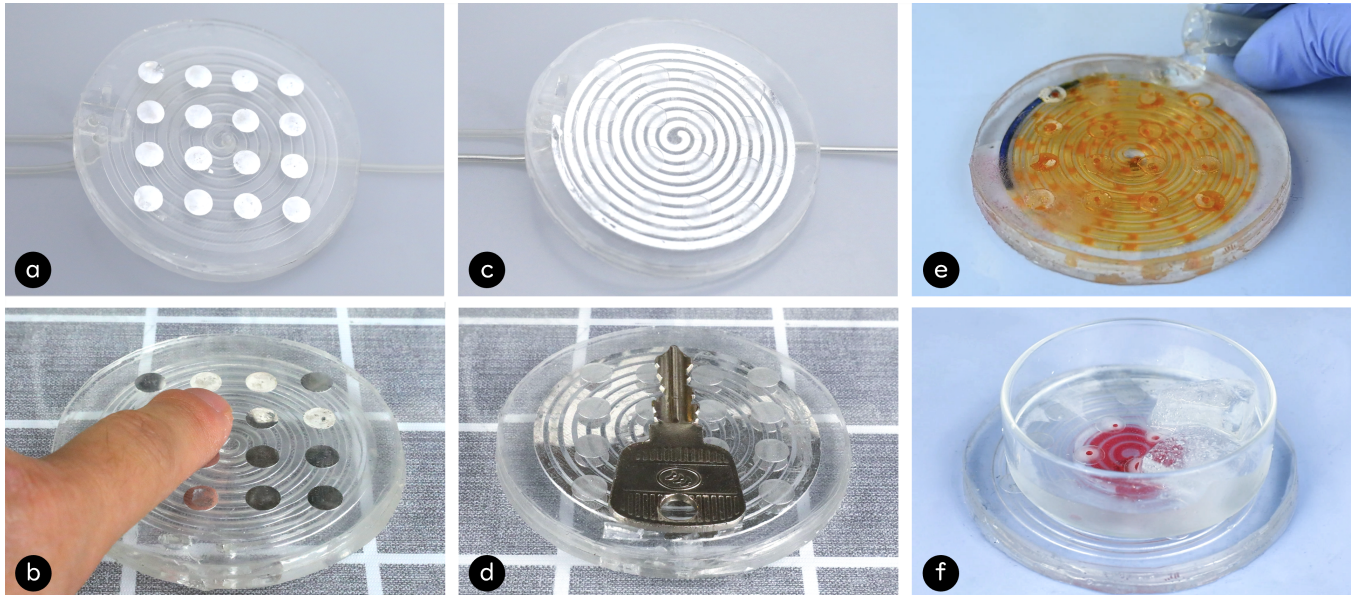


**Figure 1:** RElectrode is a multi-purpose sensing device made of microfluidic channels: a) grid electrode pattern; b) capacitive sensing; c) spiral coil pattern; d) inductive sensing; e) pH sensing; f) temperature sensing.

## ABSTRACT

In this paper, we propose a reconfigurable electrode, RElectrode, using a microfluidic technique that can change the geometry and material properties of the electrode to satisfy the needs for sensing a variety of different types of user input through touch/touchless

\*Corresponding author

Permission to make digital or hard copies of all or part of this work for personal or classroom use is granted without fee provided that copies are not made or distributed for profit or commercial advantage and that copies bear this notice and the full citation on the first page. Copyrights for components of this work owned by others than ACM must be honored. Abstracting with credit is permitted. To copy otherwise, or republish, to post on servers or to redistribute to lists, requires prior specific permission and/or a fee. Request permissions from permissions@acm.org.

CHI '21, May 8–13, 2021, Yokohama, Japan

© 2021 Association for Computing Machinery.

ACM ISBN 978-1-4503-8096-6/21/05...\$15.00

<https://doi.org/10.1145/3411764.3445652>

gestures, pressure, temperature, and distinguish between different types of objects or liquids. Unlike the existing approaches, which depend on the specific-shaped electrode for particular sensing (e.g., coil for inductive sensing), RElectrode enables capacity, inductance, resistance/pressure, temperature, pH sensings all in a single package. We demonstrate the design and fabrication of the microfluidic structure of our RElectrode, evaluate its sensing performance through several studies, and provide some unique applications. RElectrode demonstrates technical feasibility and application values of integrating physical and biochemical properties of microfluidics into novel sensing interfaces.

## CCS CONCEPTS

- Human-centered computing → Interaction devices.

## KEYWORDS

capacitive and inductive sensing, object recognition, gesture, microfluidics

### ACM Reference Format:

Wei Sun<sup>1,2</sup>, Yanjun Chen<sup>1</sup>, Simon Zhan<sup>4</sup>, Teng Han<sup>1,3</sup> and Feng Tian<sup>1,3</sup>, Hongan Wang<sup>1</sup>, Xing-Dong Yang<sup>5</sup>. 2021. RElectrode: A Reconfigurable Electrode For Multi-Purpose Sensing Based on Microfluidics. In *CHI Conference on Human Factors in Computing Systems (CHI '21), May 8–13, 2021, Yokohama, Japan*. ACM, New York, NY, USA, 12 pages. <https://doi.org/10.1145/3411764.3445652>

## 1 INTRODUCTION

Adoption of smart sensors led to the evolution of human-computer interfaces giving rise to a wide variety of new applications such as environment / everyday object sensing [4, 25], gesture/activity recognition [23, 24, 29], and personal health monitoring [30, 44]. Among those, electronic sensors are ubiquitously applied and continue to rapidly evolve, including familiar conductive, capacitive, resistive sensing, etc. Conventional electrodes of the sensors, or electric conductors, are usually metal and used as electrically conducting medium.

Though electrodes are of various forms, their metallic and solid nature restricts modification in sensing functionalities. The pattern and material properties of an electrode are normally defined by specific sensing principles, tasks and requirements. For instance, inductive sensing has been used in metal objects detection and position [4, 5], etc. An inductor of inductive sensing typically consists of an insulated wire wound into a coil around a core, e.g., a circular spiral. Another example is capacitive sensing. Interactive applications using capacitive sensing have been shown in touch and touchless gesture input, liquid level sensing, and non-metallic object recognition [6, 12, 32, 34, 36, 37], etc. An inductor on a capacitive sensing board is usually composed of a plate capacitor or a electrode grid. Sensor patterns for inductive, capacitive and other sensing apparatus have been thoroughly researched, but switching such physical properties of an electrode on demand are rarely studied in the literature.

This paper presents RElectrode, an electrode prototype that leverages microfluidic channels and is functionally reconfigurable with simple control units. Microfluidics is a science to move and manipulate fluids precisely on a small scale. For its flexible and stretchable nature, microfluidics gains popularity in development of biochemical sensors [22]. The capabilities to alter flow parameters such as rate, temperature and geometry have been shown essential for developing microfluidic devices [40]. Inspired by these properties, this work proposed a reconfigurable microfluidic platform that allows a variety types of electronic and biochemical sensing on a single board. With the designed microstructure, RElectrode is able to reconfigure the pattern (i.e., a circular spiral, an electrode grid, or both) and material (i.e., liquid metal, red ink) of the sensor (Figure 1). With such unique capabilities, RElectrode can be immediately reconfigured, acting as an inductive sensor, capacitive sensor, resistive pressure sensor, thermal sensor and pH sensor.

These novel functions of RElectrode allow us to explore interaction based on multi-purpose sensing.. We demonstrate that RElectrode can be used for contextual interactions, being able to

recognize both metallic and non-metallic objects. It can support gesture interactions, including contact and mid-air hand input such as touch (with pressure) and swipe. Additionally, it integrates a liquid channel, resulting in unique characteristics that cannot be obtained with conventional electrodes: monitoring thermal and pH values. RElectrode was made based on standard soft lithography techniques. With a series of evaluations, we show that RElectrode is easy to adapt and reliable in performing the sensing functions. RElectrode demonstrates a feasible way to fabricate electronic sensors with reconfigurable functions.

This paper made the following contributions: i) RElectrode as the first functionally reconfigurable sensor on a chip based on microfluidics; ii) structural design to achieve agile switch between a circular spiral type sensor and an electrode grid type sensor; iii) validation of using RElectrode for the compound measurement of inductive, capacitive, pressure, temperature and pH values; iv) example scenarios to demonstrate the advantage of RElectrode in interaction design.

## 2 RELATED WORK

RElectrode is a microfluidic platform that adapts to multi-purpose sensing. Here we looked into previous work on object and gesture sensing interfaces, and recent progress in electrode design and fabrication. We also reviewed sensors and actuators based on microfluidics.

### 2.1 Electrical Sensing Interface

Various electric sensing techniques have been used to innovate the design of advanced interfaces. A rich set of previous work looked into novel ways to enable touch and gesture input via electromagnetic [13, 47, 48], radio frequency [8], as well as bioelectric signals [2, 19, 31, 35]. Zhang et al. [46] leveraged the principle of Electrical Impedance Tomography (EIT) for hand gesture sensing, with surface electrodes attached around a user's arm. Hsieh et al. [8] developed 2D touch pad based on the ultra-high frequency RFID. Wu et al. [42] showed that touchless swipe gestures are possible on interactive fabrics using Doppler motion sensing.

Recently there is growing interest in deploying the sensing function in smart object and activity recognition. Capacitive sensing has been shown to be effective in detecting and measuring proximity, pressure, position and displacement, humidity and fluid level [21]. The electrodes can be embedded or integrated into flexible conductive surfaces to enrich its applying scenarios. For instance, Wu et al. [42] made capacitive sensing enabled fabric by sewing patterned electrodes on it. Resistant sensing is responsive to an applied force, pressure, and mechanical stress, and is thus often used to detect plastic deformation with a given material [38]. Aigner et al. [1] presented an embroidered way to implement resistive textile sensor patches on top of existing weaves or knits. Inductive sensing has been widely used to measure position or speed. It induces eddy current to conductive objects, especially metallic ones, and has been shown effective in contextual aware interactions [4, 5], e.g., object detection and recognition.

RElectrode got inspired by these works on developing smart sensing interfaces, e.g., gesture and context-aware interactions. Its

innovation focuses on enabling multi-purpose sensing with a reconfigurable electrode, enriching proposed applications as well as supporting novel sensing capabilities beyond conventional electrodes.

## 2.2 Electrode Design, Material and Fabrication

The electrode material and patterns are essential to the sensor's function and performance to match specific applications. For instance, a piezo electrode is of various patterns such as solid, wrap-around, side tab, insulation band, bull's-eye, and custom-designed ones [41]. The electrodes of the projected capacitive touch panel are usually made of indium or fluorine tin oxide due to their high electrical conductivity and concurrent high transparency. The electrode lines are coated on each side of a dielectric layer, horizontally and vertically respectively. Typically, they are patterned in rectangular or interlocking diamonds ways to improve touch sensitivity [16]. The inductive sensor senses the change in inductance caused by the movement of a conductive target through the sensor's AC magnetic field, thus the inductor shape is an important characteristic as it determines the shape of the generated magnetic field [14]. A circular spiral generates a more symmetrical magnetic field than other shapes. For other applications, different shapes may be more suitable. For example, rectangular coils can be used to sense accurate movement of the target object [14]. As the electrodes are typically made of conductive material, e.g., copper, different sensors can barely used together, otherwise inducing mutual affect on the generated signals.

Like typical circuits, electrodes are manufactured by rigid metallic material like copper. Recent breakthroughs in the area of stretchable electronics open up new avenues to design and manufacture flexible electrodes and other electronic components based on nanoscale materials, organic materials, and microfabrication, suggesting the potential for broader applications [33]. Meanwhile, researchers have experimented with integrating electronic components with textiles and produced a fabric-based electrode to help enhance the sensing capabilities of everyday objects [23, 24, 27–29].

RElectrode is the first attempt to design and fabricate functionally reconfigurable electrode (e.g., shape and material) based on microfluidic techniques.

## 2.3 Microfluidics Sensor

The field of microfluidics has grown enormously in the past decade, providing integrated platforms for the development of portable, easy-to-use, and sensitive lab-on-a-chip (LOC) devices for real-time detections in areas ranging widely from physics to chemistry to biotechnology to microelectronic [22]. Researchers have invented microfluidic based biosensors for dynamic sweat secretion analysis[11], rapid detection of salmonella in food [10], epidermal pH monitoring [39], and diabetes monitoring and therapy [15], etc. Microfluidic assemblies of sensors and circuits offer the potential to revolutionize electronic system architecture, advanced manufacturing processes, and flexible hybrid semiconductor [33]. Gao et al. [3] demonstrated a microfluidic tactile diaphragm pressure sensor based on embedded Galinstan micro-channels , which is capable of heart-rate monitoring. Researchers also proposed "liquid state

electronics" where conductive liquids are embedded into elastomer microchannels to form sensors [17, 26, 45].

Potential integration of microfluidics and advanced interface design has been explored by HCI researchers in recent years. MilliMorph [18] presented a design space of creating fluidic chambers and channels at millimeter scale for tangible actuated interfaces. Later, Mor et al. [20] utilized fluidic channels to design venous structures that respond to deformation by mechanical inputs from the user. Microfluidic techniques have also been used to design on-skin haptic interfaces, such as shown in HapBead [7].

This work exploited another characteristic of microfluidics, that the directed transport of minute volumes of liquids can be precisely controlled and the liquids in the channels can be switched. An innovative method has been provided to make the sensor have a unique feature that cannot be obtained by traditional devices: functional reconfigurability.

## 3 SHAPE-RECONFIGURABLE ELECTRODE

We propose RElectrode as a new sensing interface for use of multiple purposes. Different electrode patterns can be achieved by altering the flow path, while the liquid can be switched to support both electronic and biochemical sensing. This section outlines the design of the microfluidic structure to direct the flow path, and in our case, it is capable of transforming from a grid pattern to a spiral pattern, and vice versa. In other words, RElectrode supports both capacitive and inductive sensing on demand. Additionally, the compound electrode pattern enables the device to detect resistance, as well as thermal and pH values.

### 3.1 Principle & Design

The RElectrode design starts at a basic unit as illustrated in Figure 2. The key concept involves interconnected flow channels and grid chambers. The structures above are the grid chambers, while the structure below is the flow channel of the microfluidic setting. **The tunnels in-between connect those two structures. Filling the structures in different ways (i.e., the channel only, grid chamber only, both) reconfigures the status of the electrode.** A dedicated driving unit manipulates the liquid flow, as well as the air inside the chambers. Indeed, the air inside the chamber balances the pressure and prevents the liquid to flow in. Only when the chamber is vacuumed, the liquid flow can fill the chamber. We leveraged this phenomenon and designed the operation logic as follows:

To fill the channel only, the driving unit pushes the liquid from the inlet and draws it from the outlet simultaneously (Figure 2a); To fill both the channel and the grid chamber, the unit first extracts air from structures to create a relative vacuum space, and then injects the liquid that will fill up both the channel and the grid chamber (Figure 2c). **To fill the grid chamber after the state is shown in Figure 2c, a different insoluble liquid (used as the cleaning liquid) is injected into the channel, with relatively small pumping and drawing force from the inlet and outlet, respectively. This causes the membrane to deform slightly without squeezing the liquid metal out of the chamber. To empty the structures, the drawing force from the outlet gets increased, while the unit keeps pumping the cleaning liquid from the inlet.**

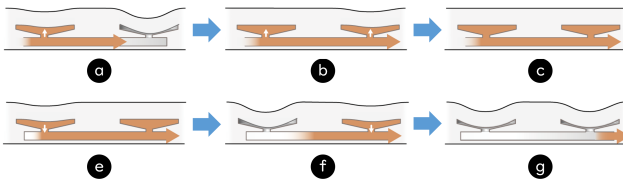


Figure 2: Procedure to fill up different part of a basic unit.

### 3.2 Circular vs. Rectangular

Circular and rectangular channel shape have been both considered, and circular shape has been selected to develop the prototype. This is because the rectangular-shaped channels have many corners, making it hard to empty the fluid inside (i.e., need more pressure from the pump) to fulfill the configurations.

### 3.3 Valve

We designed a water-driven valve based on Eco-flex material, which is more stretchable and resilient than PDMS (3). To turn on the valve, we simply pump water to the valve to stretch the Eco-flex membrane built in channel to close the gap in the channel. When turning off the valve, we cut off the air supply. The resilience of Eco-flex allows this membrane to deform back to the starting position.

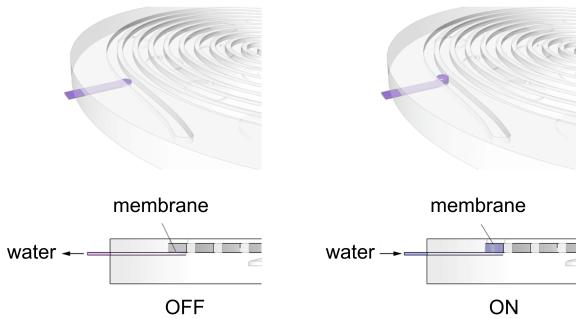


Figure 3: Schematic of the water-driven valve.

### 3.4 Liquid Metal

We conducted a few experiments on the choice of conductive liquids e.g. Ionic liquid, Mercury, liquid metal, etc. At last, liquid metal seemed to be the optimal choice. With high electrical conductivity, it can provide better sensing performance than ionic liquids. Without tremendous hazards to health, it is much safer to use than mercury. A drawback, however, is that liquid metal might form an oxidized layer when exposed to air which hampers its flowing property. To solve the problem, we applied hydrochloric acid to clean and remove this obstacle.

## 4 RELECTRODE PROTOTYPE

The prototype of RElectrode includes two parts: the electrode and the fluid driving unit. It is capable of altering the liquid inside the channels, and directing the transport of the flow. RElectrode can be

programmable reconfigured to achieve multi-purpose sensing (i.e., inductive, capacitive, resistive, temperature and pH). This section will first discuss the form factor, the fabrication process, as well as the driving units of the prototype, and then elaborate on how the sensing functions are realized on the platform.

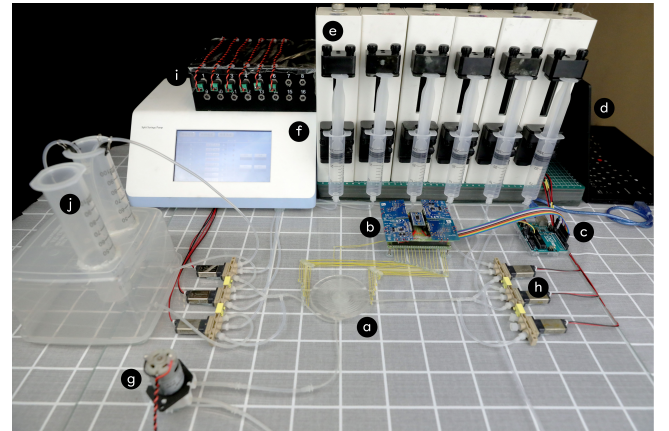


Figure 4: The overall RElectrode system presentation: a) Microfluidic chip; b) Sensor circuit board; c) Arduino Uno; d) PC; e) Split syringe pump; f) Split syringe pump controller; g) Pump; h) 3-way solenoid valve; i) valve controller; j) Fluid collection jar.

### 4.1 Form Factor

The design of RElectrode comprises a three-layer structure (Figure 5). The bottom layer, measured  $75\text{mm} \times 2\text{mm}$  thickness, embeds the circular spiral-shaped channel (i.e., flat coil), whose cross-section is  $2\text{mm}$ . This allows the liquid metal and the ink to move freely inside the channel. When filled with liquid metal, the coil electrode is of outer diameter  $60\text{mm}$ , 10 turns, and spacing between traces of  $1\text{mm}$ . The middle layer consists of interconnection tubes, measured  $1.5\text{mm}$  in height with cross-section of  $0.8\text{mm}$ . The grid chambers made the top layer. Each chamber is a cylinder with a diameter of  $7\text{mm}$  and a height of  $1\text{mm}$ . The overall thickness of the device is  $6\text{mm}$ . This is based on the spiral patterned layer ( $2\text{mm}$ ) plus the grid chamber patterned layer ( $3\text{mm}$ ) plus the superstrate ( $1\text{mm}$ ). The device is of round shape, measured  $75\text{mm}$  in diameter.

### 4.2 Fabrication

The prototype is fabricated by the standard soft lithography techniques while part of the fabrication sequence and process is improved due to the design characteristics of the device. The SU-8-Si masters for polydimethylsiloxane (PDMS) spiral-channel and grid-pad casting were designed using L-Edit software and fabricated by photolithography (Figure 6a). For each of them, a 4-inch silicon wafer was coated with SU-8 2150 photo-resist and soft-baked at  $65^\circ\text{C}$  for 10 minutes and  $95^\circ\text{C}$  for 2 hours, respectively. The photo-resist was patterned by Karl Suss MA6 Contact Aligner, followed by UV exposure ( $600\text{mJ}$  at  $365\text{nm}$ ) with a photo-mask. After exposure, a post-exposure bake was applied at  $65^\circ\text{C}$  for 5 minutes and

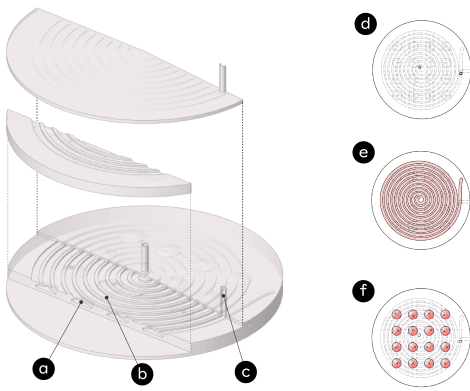


**Figure 5: Structure Design of RElectrode:** a) grid chamber, b) spiral channel, c) pipe inlet and outlet, d) empty state, e) coil only state, f) grid electrode state.

at 95°C for 30 minutes, respectively. Finally, a patterned wafer was developed in SU-8 developer for 30 minutes.

Next, PDMS (Dow and Corning's Sylgard 184) with A cross-linker/curing agent B = 10:1 was used to cast and mold the devices. The ratio was determined empirically to maintain a balanced rigidity level of the final produced PDMS layers. Eco-Flex, another commonly used substrate material for flexible electronics manufacturing, has also been considered. However, the Eco-Flex layers were found to be less rigid to stand for the flow of pressurized liquid or the shape recovery. The PDMS was stirred in a flask for over 5 minutes until visually milky with tiny air bubbles to ensure thorough mixing. The prepared PDMS was then cast into the SU-8-Si master and degassed in a vacuum desiccator for 10 minutes to remove the air bubbles. The clean and transparent PDMS was cured in an oven (85°C for 3 hours), form into a thin layer of film which can be peeled away easily from the mold (Figure 6c). So far, both the spiral patterned layer and the grid-patterned layer were ready. The superstrate was developed in the same way using a smooth silicon wafer.

Interconnect tinned copper wire was bonded neatly on the substrates, covered with thin membranes (Figure 6d). Next, the substrates and the superstrate need to be bonded permanently to provide strong barriers against internal liquid pressure (Figure 6i). The PDMS layers were exposed to oxygen plasma (Ming Heng, PDC-MG) for 60 seconds for activation. Then the activated PDMS surface was placed on another PDMS layer as soon as possible to form a permanent bond. A post-bake (55°C hours) is essential to increase the success rate. At last, Tygon tubing was adhered to the ports using PDMS and the joint was reinforced by the post-bake procedure.

In our work, soft lithography techniques and devices were adopted to ensure surface smoothness, size precision, and durability. There are other fabrication possibilities. 3D printing, as an alternative method, has been tested at the early prototyping stage. Differently, another fabrication process has been provided by 3D

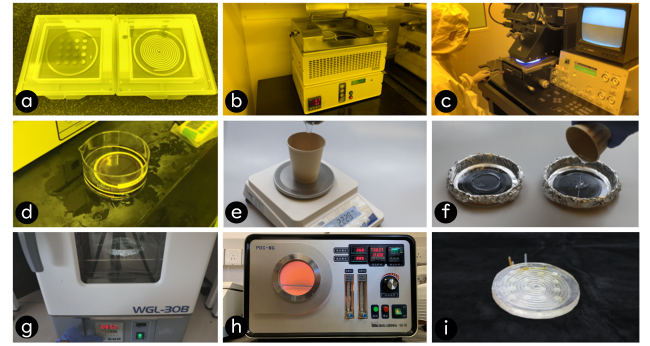


**Figure 6: Fabrication process of RElectrode (main steps):** a) mold for each mask; b) bake the SU-8; c) lithography; d) develop the pattern; e) prepare PDMS mix Sylgard 184; f) pour the PDMS into the mold; g) cure the PDMS; h) plasma bonding; i) RElectrode.

printing; PDMS (Dow and Corning's Sylgard 184) with A cross-linker/curing agent B = 10:1 was used to cast and mold the molds, and copper wire was interconnected tinned.

### 4.3 Fluid Driving Unit

The RElectrode prototype consists of a customized control circuit (Figure 7), driven by a dedicated microfluidic pumping unit. Specifically, three reservoirs are used to store liquid metal, hydrochloric acid solution ( $w(CL) = 20\%$ ), and red ink, respectively. The selected liquid is pumped to a group of 2 solenoid valves (DN 1.2mm, up to 3bar, opening/closing 3ms) connected to the inlet of the device. Another two solenoid valves are used to control the outlet of the flow, to transport the liquid to three new reservoirs, one for each liquid as well. The pressure pumps and the valves are controlled by a Python application. We modulated the push/pull and open/close switch through the inlet and outlet, to create electrodes of various geometry and material properties on RElectrode.

To avoid switching and refilling liquid frequently, we devised a liquid circulation system based on microfluidic flow switch matrices (EVEFLOW MUX) and a whisper valve. This valve has three ports and on/off two states. As Figure 7 shows, when the valve is on, B and C are opened; when valve is closed, A and B are opened. In the injection terminal, we connect both liquid metal, hydrochloric acid, and other required liquids to ports B. At the "ON" state, we can inject required liquid to the microfluidic channel connected to Port A. At the "OFF" state, the refill process can be completed by using an individual syringe through Port C. At the exit terminal, a similar logic applies. Syringes connect to microfluidic channel through Port A, "ON" state, to extract remaining liquid inside the channel. Through Port C, in the "OFF" state, the syringe can empty used liquid to reservoir for future possible reuses. Each liquid has its own reservoir, except for liquid metal and hydrochloric acid. For their distinct properties and reactions, liquid metal sinks to bottom and hydrochloric acid floats at the top within a reservoir container. Thus, we connect liquid metal input and hydrochloric acid input syringe respectively to the bottom and the top.

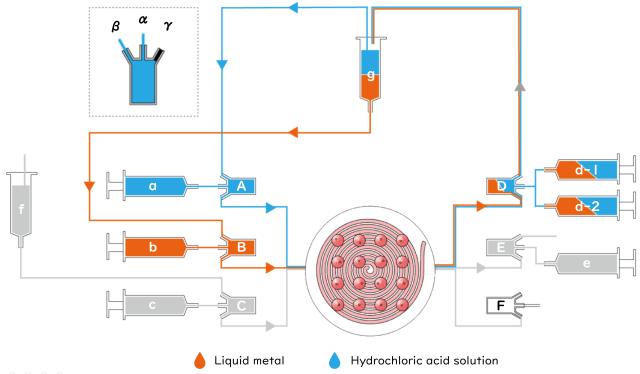


Figure 7: Schematic of the driving unit.

## 5 SENSING CAPABILITIES

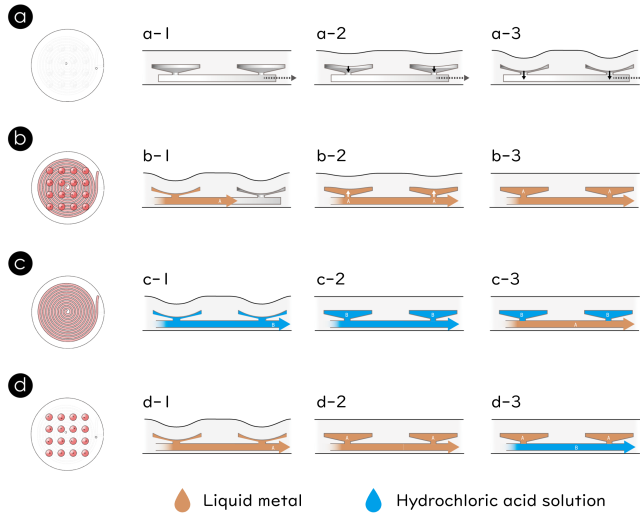


Figure 8: Configurations of different states of RElectrode: a) empty; b) both; c) spiral coil; d) grid electrodes.

Given the capabilities of changing the geometry and material properties of the electrode, RElectrode satisfies the need for sensing a variety of different types of user input through touch/touchless gestures, pressure, temperature, as well as distinguish between different types of objects or liquids.

### 5.1 Inductive Sensing

RElectrode functions as an inductive sensor when it changes to the spiral pattern. Filled with liquid metal, it has no difference from a flat coil inductor. Filling up this spiral shape, we follow the principle discussed in Section 3.1. The start and the endpoints of the spiral are connected with wires (Figure 9). As illustrated in Figure 8c, we first inject hydrochloric acid to fill up the channel and the grid chamber. Then liquid metal gets pumped in to push hydrochloric acid in the spiral channel away. Thus, we can keep liquid from accidentally

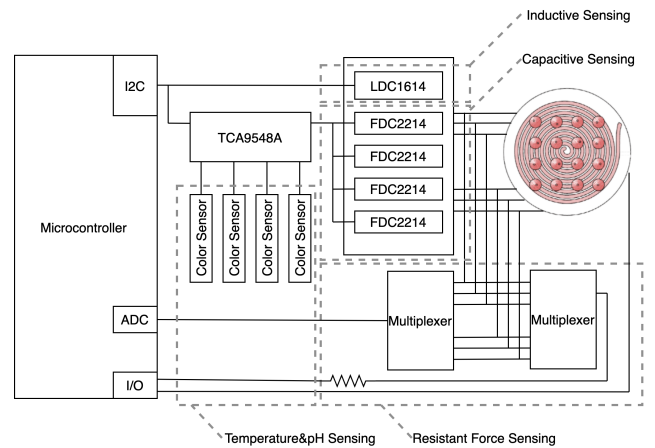


Figure 9: A schematic view of the sensing system.

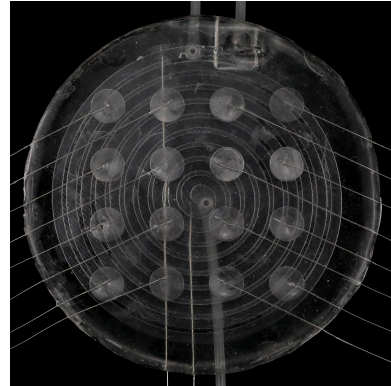


Figure 10: Overview of wire connection on microfluidic chip.

entering the grid chambers. Paralleled with a capacitor the device forms an L-C tank oscillator, which can be used to generate an AC magnetic field. Whenever a conductor gets close, eddy currents are induced on the conductor's surface. That induced currents will flow in a manner to oppose the magnetic field, which weakens the original magnetic field. An inductive-to-digital converter can be used to measure the shift in resonance. Inductive sensing has been used to develop contextual interactions [5], e.g., metal object recognition. Here, we demonstrate RElectrode can be used in a similar way via inductive sensing. RElectrode is connected to an LDC1614 evaluation board<sup>1</sup>, which fulfills the functional needs to establish inductive sensing.

### 5.2 Capacitive Sensing

Capacitive sensing is achievable when RElectrode turns to the grid pattern. To do so, we first fill both channel and the grid chamber with liquid metal. Then, via injecting hydrochloric acid into the channel that washes away liquid metal inside the channel, we can

<sup>1</sup><https://www.ti.com/tool/LDC1614EVM>

acquire 16 filled up grid chambers as shown in Figure 8 (same logistic as Section 3.1). The current implementation of RElectrode possess 16 electrodes to sense self-capacitance [43], which are organized as  $4 \times 4$  grids matrix and each has an independent wire connecting to the circuit (Figure 9). According to capacitive sensing pattern and principles [43], RElectrode can be used to identify non-metal items such as plastic, paper, fruit, etc. Besides, the capacitive sensing capabilities allow us to identify finger touch (including touch on the 16 individual points, sliding motion between those points) and gestures in the air (e.g., palm approaching, leaving the pad; sliding right and left). To support RElectrode's capacitive sensing function, we applied 4 pieces of FDC2214EVM evaluation board from Texas Instrument<sup>2</sup> to measure the values. Though using only one FDC2214 board shall be adequate for measurement purpose via routing signal to the multiplexer in circuit construction according to [5], we used 4 of them to remove circuit signal interference and to enhance the sensing stability and functionality. In order to make 4 FDC2214 chips work simultaneously, we used the TCA9548A I2C Multiplexer module<sup>3</sup> to tackle potential address conflict problems.

### 5.3 Resistant Force Sensing

RElectrode can be used as a resistant force sensor. When the liquid metal fills both the spiral channel and the grid chambers, compression of finger on each grid will cause deformation of the surface and cross-section of the liquid metal, which results in a change in resistance. The method we applied to fill up the channel and the grids were as described in Section 3.1. Since the RElectrode's surface is soft and stretchable, when heavy-compression takes place, the deformation might block the channel lying underneath. This will cause a notable rise in voltage at that breakpoint, which can be used to justify which button being pressed at what magnitude. The system uses an Arduino Uno board to detect the voltage of each channel, and via capturing these minor changes in resistance, the RElectrode can tell which grid the user is touching or pressing, as well as derive the magnitude of the finger touch pressure. And sensing pressure using resistive sensing does not need training.

### 5.4 Temperature Sensing

RElectrode is also capable of detecting temperature by switching the liquid to red ink. At the exit of the channel, we inject red ink and an equal amount of air into the channel. As we know, the PDMS has favorable heat conductivity, the mixer of air and liquid can rapidly expand or contract with temperature changes. This thermal expansion or contraction can be captured by four TCS34725 color sensors<sup>4</sup> we applied at the outlet. As Figure 11 illustrated, there are two color sensors at each side of solenoid valve: Sensor 1 and 2 (Figure 11 Group b) to detect inflation (when temperature is above room temperature); Sensor 3 and 4 (Figure 11 Group a) to detect contraction (when temperature is below room temperature). Based on the time elapsed for liquid traveling from one sensor to the other, we can induce the current environment temperature. We used

the TCA9548A I2C Multiplexer module to fix address-conflicting problems.

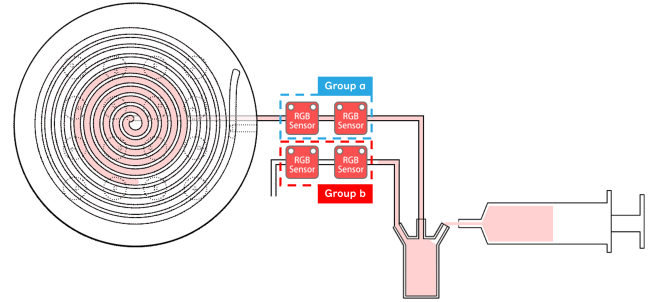


Figure 11: Temperature Sensing logic graph.

### 5.5 pH Sensing

RElectrode can be used to indicate pH value. At the inlet of the microfluidic chip, there is a small storage bud, lying behind and connected with the channel. It is designed to store indicator liquid for pH testing. The mentioned water-driven valve was located under the channel right between the storage bud and the inlet, which is designed for liquid separation. When pH indicator liquid (three different types with range:) gets injected into the channel, the water-driven valve is open. At the outlet, four TCS34725 chips, which were used in the temperature module, were applied to detect the color change in the liquid mixer, which provided corresponding pH values.

### 5.6 Data Processing

To collect data from the Arduino board, we created a Python program on the receiving computer. We used the same program to analyzes the data in two stages: data pre-processing and classification. And the program also manages the Microfluidic driving unit.

For the inductive and capacitive sensing, the raw data from the coil was smoothed using a low pass filter to reduce the fluctuations in sensor readings. For capacitive sensing, when an object gets close to the sensor, the sensor reports a  $4 \times 4$  array of capacitance values. The capacitive signal is easily interfered with by the surrounding environment. To address this issue, we subtracted background noise from the sensor reading for all data by creating a noise profile, which represented the background noise across the entire sensor. The noise profile was trained by taking the average value of all the sensor readings in a sliding time window of 5 seconds. The noise profile was constantly updated as long as there was no object detected or no threshold values exceeded. Our system only reports the presence of the object and initiate the identification process when the average of all sensors' reading is beyond the threshold value and the standard deviation is below.

For the Resistant Force Sensing, Temperature Sensing and pH Sensing, their raw data was robust enough for feature extraction. Thus we used the raw data. When changes exceed threshold values, the identification process will automatically initiate.

<sup>2</sup><https://www.ti.com/tool/FDC2214EVM>

<sup>3</sup><https://learn.adafruit.com/adafruit-tca9548a-1-to-8-i2c-multiplexer-breakout/overview>

<sup>4</sup><https://www.adafruit.com/product/1334>

## 5.7 Feature Extraction and Machine Learning

Object recognition can be powered by various Machine Learning algorithms (e.g. Random Forest, Hidden Markov Models, Convolutional Neural Network, etc). All can serve our purpose. Among them, we chose SVM, because of its reliability and accuracy in small sample data set training, which was a great fit for our demand. Features and information for training and classification were based on different data we acquired. Details are listed below.[4, 43] (Inductive sensing: Material Related Features: Mean, Variance, Max, Median. Capacitive sensing: Local Binary Pattern, Number of pixels the object covers, Number of pixels the object's edge covers, number of blobs, the average diameter of blobs, max object's pixel value of load mode, Local Maximum Numbers, median, quantiles, count above/below mean, variance, absolute energy of the object's pixel values.)

## 5.8 Gesture Detection

Gestures normally fall into two categories: one is a touch-less gesture (e.g. sliding right or left in the air) and the other is a touch gesture (e.g. pressing on the surface). With RElectrode, for touch gestures, we can identify 6 hand movements (i.e., sliding right, sliding left, sliding up, sliding down, clockwise and anti-clockwise), and touches on the 16 grid electrodes. For touch-less gestures, we can identify palm approaching and fading in the vertical direction, and moving from left to right and right to left (Figure 12). **All gestures we chose here are for feasibility test. Some more fine-grained gestures can be defined and applied in further studies.**

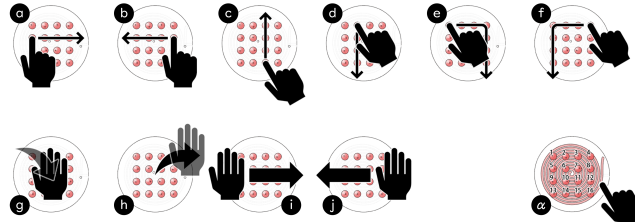


**Figure 12: Demonstrations of touch gestures from a to f; Demonstrations of touch-less gestures above pad from g to j; Demonstrations of pressing button 1-16 in  $\alpha$ .**

## 6 EVALUATIONS

We carried out a series of tests to evaluate the performance of RElectrode in different sensing scenarios.

### 6.1 Reconfiguration Cost

We test the reconfiguration time cost that mode switching from empty to spiral only, from spiral only to both, and then to grid only. The changing time costs are 4, 2, 4 secs with liquid metal on average, respectively. The setup time of temperature and pH sensing was about 3 and 2 secs, respectively, due to lower liquid density. We also test the liquid cost that fills out the spiral only, grid only and both. The average cost is 1.9, 0.4, 2.3 ml liquid, respectively.

## 6.2 Inductive Sensing



**Figure 13: The full list of tested objects: a) AirPods with wireless charging; b) credit card with chip; c) phone; d) key; e) spoon; f) card without chip; g) apple; h) peach; i) sanitizer; j) cup.**

	a	b	c	d	e	a	b	f	g	h	i	j
a	81.3	0.0	0.0	18.8	0.0	96.8	0.0	0.0	0.0	3.2	0.0	0.0
b	0.0	93.8	0.0	6.3	0.0	0.0	100	0.0	0.0	0.0	0.0	0.0
c	0.0	6.3	93.8	0.0	0.0	0.0	0.0	90.0	0.0	0.0	0.0	10.0
d	30.3	0.0	0.0	66.7	3.0	10.3	0.0	0.0	82.8	6.9	0.0	0.0
e	9.4	0.0	0.0	0.0	90.6	3.3	0.0	0.0	13.3	83.3	0.0	0.0
f	0.0	0.0	0.0	0.0	0.0	0.0	0.0	6.7	0.0	0.0	93.3	0.0
g	0.0	0.0	0.0	0.0	0.0	0.0	0.0	16.7	0.0	0.0	0.0	83.3

**Figure 14: Confusion matrix of Objects Detection by Inductive Sensing(left) and Capacitive Sensing(right).**

To evaluate the performance of inductive sensing, we used 5 conductive objects (Figure 13 a,b,c,d,e) that are common in workplaces. Some were metallic, while others were electronic devices with built-in metallic components. The data was collected by a volunteer with the RElectrode. The volunteer was asked to place an object on the RElectrode in random orientations and locations inside the sensing area. The only instruction the volunteer was given was to ensure the object's contact area to be exposed to the RElectrode as much as possible. Sample data was collected 30 times per object, and the orders were random.

Overall, our system yields an accuracy of 85.2% ( $SD = 10.34$ ) by using 10-fold cross-validation. The confusion matrix of the study result showed that 3 out of the 5 tested objects achieved an accuracy higher than 90% (Figure 14 left).

## 6.3 Capacitive Sensing

In this section, we present the performance of capacitive sensing. The evaluation of the sensor was divided into two parts: non-conductive object detection, touch and touchless gesture detection. These detections evaluated the capacitive sensor using 10-fold cross-validation.

We chose 7 objects (Figure 13 a,b,f,g,h,i,j), containing non-conducting materials, appeared on our work-desk within our grab. Asked to randomly place an object at the center of the RElectrode, volunteers collected data 30 times for the 7 objects individually. Overall, our system yields an accuracy of 89.9% (SD = 6.53) for the 7 object detection result. The confusion matrix of the study result showed that 4 out of the 7 tested objects achieved an accuracy higher than 90% (Figure 14 right).

For different touch and touch-less gestures, we invited 12 volunteers in the sampling process, ranging from 23 years old to 28 years old with an average of 25.25 years old. Each individual repeated every gesture 30 times to acquire reliable data at random order. The confusion matrix of the study result showed that our system yielded an accuracy of 91.7% (SD = 3.97) for the 10 gestures (Figure 15).

	<b>a</b>	<b>b</b>	<b>c</b>	<b>d</b>	<b>e</b>	<b>f</b>	<b>g</b>	<b>h</b>	<b>i</b>	<b>j</b>
<b>a</b>	85.0	0.0	0.0	1.0	12.5	0.5	0.0	0.5	0.0	0.5
<b>b</b>	0.0	96.8	0.0	0.0	0.5	0.5	0.0	0.5	1.4	0.5
<b>c</b>	2.3	0.0	93.1	0.0	0.0	0.0	0.9	0.9	1.4	1.4
<b>d</b>	1.0	0.5	0.5	88.8	0.0	9.3	0.0	0.0	0.0	0.0
<b>e</b>	10.5	0.0	0.9	0.0	85.8	1.4	0.9	0.0	0.5	0.0
<b>f</b>	0.5	0.0	0.5	7.7	0.0	91.4	0.0	0.0	0.0	0.0
<b>g</b>	0.0	0.5	0.0	0.0	0.0	0.0	92.9	0.0	2.0	4.5
<b>h</b>	0.5	0.9	0.0	0.0	0.0	0.5	0.0	97.2	0.5	0.5
<b>i</b>	0.0	2.2	0.0	0.0	1.3	0.0	3.0	0.4	90.9	2.2
<b>j</b>	0.0	0.0	0.0	0.0	0.0	0.0	4.8	0.0	0.5	94.8

Figure 15: Confusion matrix of gesture detection.

#### 6.4 Resistant Force Sensing

Resistance testing can be used to identify different button events and access to touching magnitude. Besides, when we gently touch on those 16 grid reservoirs, the button event can also be triggered. As we introduced in Section 5.3, this touch will cause a change in the cross-section of the grid reservoir and channel, which results from changes in resistance. Therefore, in resistant force sensing, RElectrode implements 16 button touch events. This resistance-based testing makes tests on individual grid pixels simultaneously possible and can be applied to multi-touch detection scenarios. The data was collected 30 times per button by a volunteer(the orders were random). Our system yields an accuracy of 97.9% (SD = 3.1) for 16 press button (Figure 16).

#### 6.5 Temperature Sensing

The liquid (i.e., red ink) in RElectrode’s channel responds to the temperature change by contraction and expansion. Therefore, it can be known that, compared with the default temperature (such as room temperature), the hotter/colder the target object, the faster the system response. To avoid the left-over effect from a previous test, we extruded the affected air inside the channel and pumped in fresh air before taking a new measurement. Next, we pumped

	<b>1</b>	<b>2</b>	<b>3</b>	<b>4</b>	<b>5</b>	<b>6</b>	<b>7</b>	<b>8</b>	<b>9</b>	<b>10</b>	<b>11</b>	<b>12</b>	<b>13</b>	<b>14</b>	<b>15</b>	<b>16</b>
<b>1</b>	100.0	0.0	0.0	0.0	0.0	0.0	0.0	0.0	0.0	0.0	0.0	0.0	0.0	0.0	0.0	0.0
<b>2</b>	0.0	100.0	0.0	0.0	0.0	0.0	0.0	0.0	0.0	0.0	0.0	0.0	0.0	0.0	0.0	0.0
<b>3</b>	0.0	0.0	100.0	0.0	0.0	0.0	0.0	0.0	0.0	0.0	0.0	0.0	0.0	0.0	0.0	0.0
<b>4</b>	0.0	0.0	0.0	100.0	0.0	0.0	0.0	0.0	0.0	0.0	0.0	0.0	0.0	0.0	0.0	0.0
<b>5</b>	0.0	0.0	0.0	0.0	93.3	0.0	0.0	0.0	0.0	0.0	0.0	0.0	0.0	6.7	0.0	0.0
<b>6</b>	0.0	0.0	0.0	0.0	0.0	100.0	0.0	0.0	0.0	0.0	0.0	0.0	0.0	0.0	0.0	0.0
<b>7</b>	0.0	0.0	0.0	0.0	0.0	0.0	96.8	3.2	0.0	0.0	0.0	0.0	0.0	0.0	0.0	0.0
<b>8</b>	3.3	0.0	0.0	0.0	0.0	0.0	3.3	90.0	0.0	3.3	0.0	0.0	0.0	0.0	0.0	0.0
<b>9</b>	0.0	0.0	0.0	0.0	0.0	0.0	0.0	0.0	100.0	0.0	0.0	0.0	0.0	0.0	0.0	0.0
<b>10</b>	0.0	0.0	0.0	0.0	0.0	0.0	0.0	0.0	3.3	93.3	0.0	0.0	3.3	0.0	0.0	0.0
<b>11</b>	0.0	0.0	0.0	0.0	0.0	0.0	0.0	0.0	0.0	96.7	0.0	3.3	0.0	0.0	0.0	0.0
<b>12</b>	0.0	0.0	0.0	0.0	0.0	0.0	0.0	0.0	0.0	0.0	100.0	0.0	0.0	0.0	0.0	0.0
<b>13</b>	0.0	0.0	0.0	0.0	0.0	0.0	0.0	0.0	0.0	3.3	0.0	96.7	0.0	0.0	0.0	0.0
<b>14</b>	0.0	0.0	0.0	0.0	0.0	0.0	0.0	0.0	0.0	0.0	0.0	0.0	100.0	0.0	0.0	0.0
<b>15</b>	0.0	0.0	0.0	0.0	0.0	0.0	0.0	0.0	0.0	0.0	0.0	0.0	0.0	0.0	100.0	0.0
<b>16</b>	0.0	0.0	0.0	0.0	0.0	0.0	0.0	0.0	0.0	0.0	0.0	0.0	0.0	0.0	0.0	100.0

Figure 16: Confusion matrix of resistant force sensing results.

Table 1: Temperature Sensing

Temperature(°C )	90	80	70	60	50	0
Time (s)	4.5	5.6	6.2	7.6	10.5	9

in a certain amount of red ink liquid from the outlet side of the channel (described in Section 5.4 and Figure 11). In this test, we placed several cups of water of known temperature (Table 1) on top of the sensor, and monitored the responses. The RGB sensor was used to detect the signal. Based on the physical distance between the pair of sensor and the system reaction lay-back table, we were able to measure the reaction time for temperatures, and infer the temperate values.

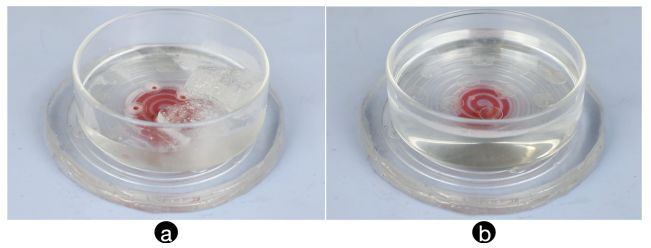


Figure 17: a) cold target object; b) hot target object.

#### 6.6 pH Sensing

To make sure there was no oxidized liquid metal left in the channel, we applied hydrochloric acid to clean the channel and pumped in the air to dry the channel. These preparation steps took about 30 seconds.

As known, increasing the speed of pH indicator liquid injection can enhance the *Siphon Effect* taken place within the channel. This can make the mixer fully react to the testing liquid. However, this will raise two questions:

- More pH indicator liquid is needed for the test, which causes unnecessary waste.
- The fast flow rate might impede the detection of the color sensors.

Thus, we chose the slow-flowing mode for pH detection (the driving unit pumps slowly), and it took about 15 seconds to obtain the results.

## 6.7 Compound Sensing

There are large amounts of objects composed of conductive and non-conductive materials in daily life. Using any sensor (such as an inductive or capacitive sensor) alone for detection will result in an object identification error that cannot acquire all-around information. For example, using capacitive sensing to identify whether certain AirPods supports wireless charging is very difficult. However, with aid from inductive sensing, these problems can be solved, since the metallic information can be obtained. Besides, RElectrode can identify objects from some complicated compounds (e.g., a spoon in a mug). This capability cannot be achieved by using any sensor alone

In the experiment, we collected both inductance and capacitance of 6 objects in random order 30 times each. Applying the method we discussed above [Section 5.6](#) and combining both inductive and capacitive properties, we conduct SVM classification on a single dimension. The identification accuracy is 69.2%, 62.0% for inductive sensing and conductive sensing, respectively, and the classification result is 77.3%(SD = 15.4) with RElectrode. We found that the cup and the plastic card were hard to tell by the system. The possible reason is that the selected feature was more sensitive to the comparison of metal and non-metal objects, but not well suited to distinguish two non-metal objects. This could be improved in the future.



**Figure 18:** a) AirPods with wireless charging; b) AirPods without wireless charging; c) credit card with chip; d) credit card without chip; e) cup; f) spoon in cup.

## 7 DISCUSSION

RElectrode presents a feasible technical solution to design and fabricate an electrode for multiple purpose sensing. The key concept involves the design of a micro channel-chamber structure to direct the liquid flow, such that the electrode pattern can be reconfigured in a quick and easy way. It turns out RElectrode works efficiently

	a	b	c	d	e	f
a	87.1	12.9	0.0	0.0	0.0	0.0
b	13.3	86.7	0.0	0.0	0.0	0.0
c	0.0	3.3	96.7	0.0	0.0	0.0
d	0.0	0.0	0.0	66.7	23.3	10.0
e	0.0	3.3	0.0	36.7	50.0	10.0
f	0.0	0.0	0.0	0.0	23.3	76.7

**Figure 19:** a) RElectrode can be used for compound sensing, e.g., recognize a spoon in a cup; b) Confusion matrix of compound sensing results.

and reliably on the proposed sensing capabilities, and can help to envision novel contextual and gestural interaction scenarios ([Figure 11](#)).

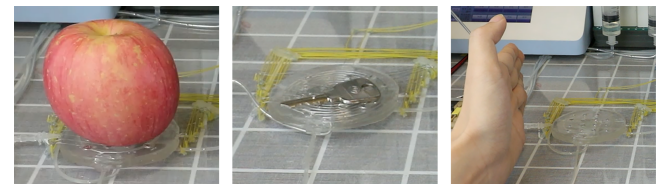


**Figure 20: Object and gesture detection**

As demonstrated, RElectrode is sensitive to pressure applied on top of the device. Owing to the flexible nature of the material, subtle changes in the shape would cause the flow of liquid metal to change in resistance. Pressure change can be detected, but how the applied pressure (e.g., weight) would affect the other sensing abilities has to be explored. When fabricating the prototype, we found the rigid/flexible level of the material has to be carefully determined. The material selected should be sensitive for pressure detection while stable enough.

The current design of RElectrode is relevantly large in size. This is due to the consideration that downsizing the device will cause changes in the way the fluids pass through the channels. Surface tension force would play a dominant role, making it hard for liquid metal to pass through the microscale tubes. This brings new challenges to liquid material selection. Currently, RElectrode has to be used on a flat surface, otherwise additional liquid pressure has to be applied to counterbalance the effect of gravity.

RElectrode's superstrate is non-conductive due to the property of PDMS. The material can be made conductive, e.g., by mixing it with carbon nanopowder, to be applicable for direct contact sensing. This would help to enrich the sensing capabilities and broaden the use scenarios of RElectrode. In this work, we took standard lithography techniques to fabricate the device. Casting the mold, on the other hand, can be done with regular 3D printers. In this way, it provides possibilities to DIY the RElectrode. We believe

this will help to improve the design and exploring the potential of RElectrode to a large extent.

As RElectrode is made of PDMS, it is normally flexible, thus could be potentially used on the body for intelligent on-body sensing and health care monitoring. To do so, either the substrate or the superstrate of the device shall be made shielded to avoid interruption of capacitive or inductive sensing. RElectrode can be easily sealed, thus could be used in extreme situations such as under the water. Such potential shall be further explored in the future.

The device is currently driven by a dedicated pumping unit for precise control of the liquid flow. Next, we would like to provide alternative driving methods that would make RElectrode more self-contained and portable. This can be achieved by developing fluid self-actuating mechanisms, which have been broadly explored in the area of microfluidics.

**While our current implementation uses external devices to sense pH and temperature, it is completely feasible to make the entire system self-contained in the future by embedding a miniature optical sensor (e.g., fiber-based ones [9]) in the microfluidic channels. This way, objects are not required to be transparent.**

## 8 CONCLUSION

RElectrode is a multi-purpose sensing platform made of microfluidic channels. It is functionally reconfigurable via altering the pattern and liquid flow inside the channel. We describe the principle and fabrication process, and demonstrate that RElectrode is novel in the way that it serves as an inductive, capacitive, resistive pressure, thermal and pH sensor on a single chip. RElectrode enables novel interaction scenarios, e.g., being able to recognize both metallic and non-metallic objects and support touch and gesture input. RElectrode demonstrates a feasible way to fabricate electronic sensors with reconfigurable function.

## ACKNOWLEDGMENTS

This work was supported by National Natural Science Foundation of China (Grant No. 61972387). We would like to thank the reviewers for their constructive comments and the participants in the user study.

## REFERENCES

- [1] Roland Aigner, Andreas Pointner, Thomas Preindl, Patrick Parzer, and Michael Haller. 2020. Embroidered Resistive Pressure Sensors: A Novel Approach for Textile Interfaces. In *Proceedings of the 2020 CHI Conference on Human Factors in Computing Systems* (Honolulu, HI, USA) (*CHI '20*). Association for Computing Machinery, New York, NY, USA, 1–13. <https://doi.org/10.1145/3313831.3376305>
- [2] Christoph Amma, Thomas Krings, Jonas Böer, and Tanja Schultz. 2015. Advancing Muscle-Computer Interfaces with High-Density Electromyography. In *Proceedings of the 33rd Annual ACM Conference on Human Factors in Computing Systems* (Seoul, Republic of Korea) (*CHI '15*). Association for Computing Machinery, New York, NY, USA, 929–938. <https://doi.org/10.1145/2702123.2702501>
- [3] Yuji Gao, Hiroki Ota, Ethan W Schaler, Kevin Chen, Allan Zhao, Wei Gao, Hossein M Fahad, Yonggang Leng, Anzong Zheng, Furui Xiong, et al. 2017. Wearable microfluidic diaphragm pressure sensor for health and tactile touch monitoring. *Advanced Materials* 29, 39 (2017), 1701985. <https://doi.org/10.1002/adma.201701985>
- [4] Jun Gong, Yu Wu, Lei Yan, Teddy Seyed, and Xing-Dong Yang. 2019. Tessutivo: Contextual Interactions on Interactive Fabrics with Inductive Sensing. In *Proceedings of the 32nd Annual ACM Symposium on User Interface Software and Technology* (New Orleans, LA, USA) (*UIST '19*). Association for Computing Machinery, New York, NY, USA, 29–41. <https://doi.org/10.1145/332165.3347897>
- [5] Jun Gong, Xin Yang, Teddy Seyed, Josh Urban Davis, and Xing-Dong Yang. 2018. Indutivo: Contact-Based, Object-Driven Interactions with Inductive Sensing. In *Proceedings of the 31st Annual ACM Symposium on User Interface Software and Technology* (Berlin, Germany) (*UIST '18*). Association for Computing Machinery, New York, NY, USA, 321–333. <https://doi.org/10.1145/3242587.3242662>
- [6] Tobias Grosse-Puppendahl, Andreas Braun, Felix Kamieth, and Arjan Kuijper. 2013. Swiss-cheese extended: an object recognition method for ubiquitous interfaces based on capacitive proximity sensing. In *Proceedings of the SIGCHI Conference on Human Factors in Computing Systems*. 1401–1410. <https://doi.org/10.1145/2470654.2466186>
- [7] Teng Han, Shubhi Bansal, Xiaochen Shi, Yanjun Chen, Baogang Quan, Feng Tian, Hongan Wang, and Sriram Subramanian. 2020. HapBead: On-Skin Microfluidic Haptic Interface Using Tunable Bead. In *Proceedings of the 2020 CHI Conference on Human Factors in Computing Systems* (Honolulu, HI, USA) (*CHI '20*). Association for Computing Machinery, New York, NY, USA, 1–10. <https://doi.org/10.1145/3313831.3376190>
- [8] Meng-Ju Hsieh, Jr-Ling Guo, Chin-Yuan Lu, Han-Wei Hsieh, Rong-Hao Liang, and Bing-Yu Chen. 2019. RFTouchPads: Batteryless and Wireless Modular Touch Sensor Pads Based on RFID. In *Proceedings of the 32nd Annual ACM Symposium on User Interface Software and Technology* (New Orleans, LA, USA) (*UIST '19*). Association for Computing Machinery, New York, NY, USA, 999–1011. <https://doi.org/10.1145/3332165.3347910>
- [9] Yesl Jun, Edward Kang, Sukyung Chae, and Sang-Hoon Lee. 2014. Microfluidic spinning of micro-and nano-scale fibers for tissue engineering. *Lab on a Chip* 14, 13 (2014), 2145–2160. <https://doi.org/10.1039/c3lc51414e>
- [10] Giyoung Kim, Ji-Hea Moon, Chang-Yeon Moh, and Jong-guk Lim. 2015. A microfluidic nano-biosensor for the detection of pathogenic Salmonella. *Biosensors and Bioelectronics* 67 (2015), 243–247. <https://doi.org/10.1016/j.bios.2014.08.023>
- [11] Ahyeon Koh, Daeshik Kang, Yeguang Xue, Seungmin Lee, Rafal M Pielak, Jeonghyun Kim, Taehwan Hwang, Seunghwan Min, Anthony Banks, Philippe Bastien, et al. 2016. A soft, wearable microfluidic device for the capture, storage, and colorimetric sensing of sweat. *Science translational medicine* 8, 366 (2016), 366ra165–366ra165. <https://doi.org/10.1126/scitranslmed.aaf2593>
- [12] Brajesh Kumar, G Rajita, and Nirupama Mandal. 2014. A review on capacitive-type sensor for measurement of height of liquid level. *Measurement and control* 47, 7 (2014), 219–224. <https://doi.org/10.1177/0020294014546943>
- [13] Gierad Laput, Yang Zhang, and Chris Harrison. 2017. Synthetic Sensors: Towards General-Purpose Sensing. In *Proceedings of the 2017 CHI Conference on Human Factors in Computing Systems* (Denver, Colorado, USA) (*CHI '17*). Association for Computing Machinery, New York, NY, USA, 3986–3999. <https://doi.org/10.1145/3025453.3025773>
- [14] LDC 2015. *LDC Sensor Design*. Retrieved Sep 17, 2020 from <https://www.ti.com/lit/an/snqa930b/snqa930b.pdf?keyMatch=LDC%20SENSOR%20DESIGN&tisearch=Search-EN-everything>
- [15] Jan Lee. 1981. Transcript of question and answer session. In *History of programming languages I (incoll)*, Richard L. Wexelblat (Ed.). ACM, New York, NY, USA, 68–71. <https://doi.org/10.1145/800025.1198348>
- [16] Jeffrey Lee, Matthew T Cole, Jackson Chi Sun Lai, and Arokia Nathan. 2014. An analysis of electrode patterns in capacitive touch screen panels. *Journal of display technology* 10, 5 (2014), 362–366. <https://doi.org/10.1109/JDT.2014.2303980>
- [17] Chien-Han Lin, Chien-Kai Wang, Yu-An Chen, Chien-Chung Peng, Wei-Hao Liao, and Yi-Chung Tung. 2016. Measurement of in-plane elasticity of live cell layers using a pressure sensor embedded microfluidic device. *Scientific reports* 6 (2016), 36425. <https://doi.org/10.1038/srep36425>
- [18] Qiuyu Lu, Jifei Ou, João Wilbert, André Haben, Haipeng Mi, and Hiroshi Ishii. 2019. MilliMorph – Fluid-Driven Thin Film Shape-Change Materials for Interaction Design. In *Proceedings of the 32nd Annual ACM Symposium on User Interface Software and Technology* (New Orleans, LA, USA) (*UIST '19*). Association for Computing Machinery, New York, NY, USA, 663–672. <https://doi.org/10.1145/3332165.3347956>
- [19] Jess McIntosh, Charlie McNeill, Mike Fraser, Frederic Kerber, Markus Löchtefeld, and Antonio Krüger. 2016. EMPRESS: Practical Hand Gesture Classification with Wrist-Mounted EMG and Pressure Sensing. In *Proceedings of the 2016 CHI Conference on Human Factors in Computing Systems* (San Jose, California, USA) (*CHI '16*). Association for Computing Machinery, New York, NY, USA, 2332–2342. <https://doi.org/10.1145/2858036.2858093>
- [20] Hila Mor, Tianyu Yu, Ken Nakagaki, Benjamin Harvey Miller, Yichen Jia, and Hiroshi Ishii. 2020. Venous Materials: Towards Interactive Fluidic Mechanisms. In *Proceedings of the 2020 CHI Conference on Human Factors in Computing Systems* (Honolulu, HI, USA) (*CHI '20*). Association for Computing Machinery, New York, NY, USA, 1–14. <https://doi.org/10.1145/3313831.3376129>
- [21] Baoqing Nie, Ruya Li, Jennifer Cao, James D Brandt, and Tingrui Pan. 2015. Flexible transparent iontronic film for interfacial capacitive pressure sensing. *Advanced Materials* 27, 39 (2015), 6055–6062. <https://doi.org/10.1002/adma.201502556>
- [22] Georgia-Paraskevi Nikoleli, Christina G Siontorou, Dimitrios P Nikolelis, Spyridoula Bratakou, Stephanos Karapetis, and Nikolaos Tzamtzis. 2018. Biosensors Based on Microfluidic Devices Lab-on-a-Chip and Microfluidic Technology. In *Nanotechnology and Biosensors*. Elsevier, 375–394. <https://doi.org/10.1016/B978-0-12-813855-7.00013-1>

- [23] Alex Olwal, Jon Moeller, Greg Priest-Dorman, Thad Starner, and Ben Carroll. 2018. I/O Braid: Scalable Touch-Sensitive Lighted Cords Using Spiraling, Repeating Sensing Textiles and Fiber Optics. In *Proceedings of the 31st Annual ACM Symposium on User Interface Software and Technology* (Berlin, Germany) (*UIST '18*). Association for Computing Machinery, New York, NY, USA, 485–497. <https://doi.org/10.1145/3242587.3242638>
- [24] Alex Olwal, Thad Starner, and Gow Mainini. 2020. E-Textile Microinteractions: Augmenting Twist with Flick, Slide and Grasp Gestures for Soft Electronics. In *Proceedings of the 2020 CHI Conference on Human Factors in Computing Systems* (Honolulu, HI, USA) (*CHI '20*). Association for Computing Machinery, New York, NY, USA, 1–13. <https://doi.org/10.1145/3313831.3376236>
- [25] Athina Panopoulou, Xiaoting Zhang, Tammy Qiu, Xing-Dong Yang, and Emily Whiting. 2020. Tactile Line Drawings for Improved Shape Understanding in Blind and Visually Impaired Users. *ACM Trans. Graph.* 39, 4, Article 89 (July 2020), 13 pages. <https://doi.org/10.1145/3386569.3392388>
- [26] Yong-Lae Park, Bor-Rong Chen, and Robert J Wood. 2012. Design and fabrication of soft artificial skin using embedded microchannels and liquid conductors. *IEEE Sensors journal* 12, 8 (2012), 2711–2718. <https://doi.org/10.1109/JSEN.2012.2200790>
- [27] Patrick Parzer, Florian Perteneder, Kathrin Probst, Christian Rendl, Joanne Leong, Sarah Schuetz, Anita Vogl, Reinhard Schwedauer, Martin Kaltenbrunner, Siegfried Bauer, and Michael Haller. 2018. RESi: A Highly Flexible, Pressure-Sensitive, Imperceptible Textile Interface Based on Resistive Yarns. In *Proceedings of the 31st Annual ACM Symposium on User Interface Software and Technology* (Berlin, Germany) (*UIST '18*). Association for Computing Machinery, New York, NY, USA, 745–756. <https://doi.org/10.1145/3242587.3242664>
- [28] Patrick Parzer, Adwait Sharma, Anita Vogl, Jürgen Steimle, Alex Olwal, and Michael Haller. 2017. SmartSleeve: Real-Time Sensing of Surface and Deformation Gestures on Flexible, Interactive Textiles, Using a Hybrid Gesture Detection Pipeline. In *Proceedings of the 30th Annual ACM Symposium on User Interface Software and Technology* (Quebec City, QC, Canada) (*UIST '17*). Association for Computing Machinery, New York, NY, USA, 565–577. <https://doi.org/10.1145/3126594.3126652>
- [29] Ivan Poupyrev, Nan-Wei Gong, Shio Fukuhara, Mustafa Emre Karagozler, Carsten Schwesig, and Karen E. Robinson. 2016. Project Jacquard: Interactive Digital Textiles at Scale. In *Proceedings of the 2016 CHI Conference on Human Factors in Computing Systems* (San Jose, California, USA) (*CHI '16*). Association for Computing Machinery, New York, NY, USA, 4216–4227. <https://doi.org/10.1145/2858036.2858176>
- [30] Tyler R Ray, Jungil Choi, Amay J Bandodkar, Siddharth Krishnan, Philipp Gutzfrud, Limei Tian, Roozbeh Ghaffari, and John A Rogers. [n.d.]. Bio-integrated wearable systems: a comprehensive review. *Chemical reviews* ([n.d.]). <https://doi.org/10.1021/acs.chemrev.8b00573>, volume={119}, number={8}, pages={5461–5533}, year=[2019], publisher={ACSPublications}
- [31] Jun Rekimoto. 2001. GestureWrist and GesturePad: Unobtrusive Wearable Interaction Devices. In *Proceedings of the 5th IEEE International Symposium on Wearable Computers (ISWC '01)*. IEEE Computer Society, USA, 21. <https://doi.org/10.1109/ISWC.2001.962092>
- [32] Jun Rekimoto. 2002. SmartSkin: An Infrastructure for Freehand Manipulation on Interactive Surfaces. In *Proceedings of the SIGCHI Conference on Human Factors in Computing Systems* (Minneapolis, Minnesota, USA) (*CHI '02*). Association for Computing Machinery, New York, NY, USA, 113–120. <https://doi.org/10.1145/503376.503397>
- [33] John A Rogers, Xiaodong Chen, and Xue Feng. 2020. Flexible Hybrid Electronics. *Advanced Materials* 32, 15 (2020), 1905590. <https://doi.org/10.1002/adma.201905590>
- [34] Ilya Rosenberg and Ken Perlin. 2009. The UnMousePad: An Interpolating Multi-Touch Force-Sensing Input Pad. *ACM Trans. Graph.* 28, 3, Article 65 (July 2009), 9 pages. <https://doi.org/10.1145/1531326.1531371>
- [35] T Scott Saponas, Desney S. Tan, Dan Morris, and Ravin Balakrishnan. 2008. Demonstrating the Feasibility of Using Forearm Electromyography for Muscle-Computer Interfaces. In *Proceedings of the SIGCHI Conference on Human Factors in Computing Systems* (Florence, Italy) (*CHI '08*). Association for Computing Machinery, New York, NY, USA, 515–524. <https://doi.org/10.1145/1357054.1357138>
- [36] Martin Schmitz, Mohammadreza Khalilbeigi, Matthias Balwierz, Roman Lissermann, Max Mühlhäuser, and Jürgen Steimle. 2015. Capricate: A Fabrication Pipeline to Design and 3D Print Capacitive Touch Sensors for Interactive Objects. In *Proceedings of the 28th Annual ACM Symposium on User Interface Software and Technology* (Charlotte, NC, USA) (*UIST '15*). Association for Computing Machinery, New York, NY, USA, 253–258. <https://doi.org/10.1145/2807442.2807503>
- [37] Maximilian Sergio, Nicolo Maresi, Marco Tartagni, Roberto Guerrieri, and Roberto Canegallo. 2002. A textile based capacitive pressure sensor. In *SENSORS, 2002 IEEE*, Vol. 2. IEEE, 1625–1630. <https://doi.org/10.1109/ICSENS.2002.1037367>
- [38] Takao Someya, Tsuyoshi Sekitani, Shingo Iba, Yusaku Kato, Hiroshi Kawaguchi, and Takayasu Sakurai. 2004. A large-area, flexible pressure sensor matrix with organic field-effect transistors for artificial skin applications. *Proceedings of the National Academy of Sciences* 101, 27 (2004), 9966–9970. <https://doi.org/10.1073/pnas.0401918101>
- [39] Yanyan Tang, Li Zhen, Jingqing Liu, and Jianmin Wu. 2013. Rapid antibiotic susceptibility testing in a microfluidic pH sensor. *Analytical chemistry* 85, 5 (2013), 2787–2794. <https://doi.org/10.1021/ac303282j>
- [40] David P Taylor and Govind V Kaigala. 2020. Reconfigurable microfluidics: real-time shaping of virtual channels through hydrodynamic forces. *Lab on a Chip* 20, 10 (2020), 1720–1728. <https://doi.org/10.1039/d0lc00197j>
- [41] TUG 2017. ELECTRODE MATERIAL AND PATTERN. Retrieved Sep 17, 2020 from <http://www.noliac.com/customized-design/components/electrode-material-and-pattern/>
- [42] Te-Yen Wu, Shutong Qi, Junchi Chen, MuJie Shang, Jun Gong, Teddy Seyed, and Xing-Dong Yang. 2020. Fabriccio: Touchless Gestural Input on Interactive Fabrics. In *Proceedings of the 2020 CHI Conference on Human Factors in Computing Systems* (Honolulu, HI, USA) (*CHI '20*). Association for Computing Machinery, New York, NY, USA, 1–14. <https://doi.org/10.1145/3313831.3376681>
- [43] Te-Yen Wu, Lu Tan, Yuji Zhang, Teddy Seyed, and Xing-Dong Yang. 2020. Capacitivo: Contact-Based Object Recognition on Interactive Fabrics using Capacitive Sensing. In *Proceedings of the 33rd Annual ACM Symposium on User Interface Software and Technology*. 649–661. <https://doi.org/10.1145/3379337.3415829>
- [44] Shanshan Yao, Puchakayala Sweatha, and Yong Zhu. 2018. Nanomaterial-Enabled wearable sensors for healthcare. *Advanced healthcare materials* 7, 1 (2018), 1700889. <https://doi.org/10.1002/adhm.201700889>
- [45] Joo Chuan Yeo, Jiahao Yu, Zhao Ming Koh, Zhiping Wang, and Chwee Teck Lim. 2016. Wearable tactile sensor based on flexible microfluidics. *Lab on a Chip* 16, 17 (2016), 3244–3250. <https://doi.org/10.1039/C6LC00579A>
- [46] Yang Zhang and Chris Harrison. 2015. Tomo: Wearable, Low-Cost Electrical Impedance Tomography for Hand Gesture Recognition. In *Proceedings of the 28th Annual ACM Symposium on User Interface Software and Technology* (Charlotte, NC, USA) (*UIST '15*). Association for Computing Machinery, New York, NY, USA, 167–173. <https://doi.org/10.1145/2807442.2807480>
- [47] Yang Zhang, Gierad Laput, and Chris Harrison. 2017. Electrictk: Low-Cost Touch Sensing Using Electric Field Tomography. In *Proceedings of the 2017 CHI Conference on Human Factors in Computing Systems* (Denver, Colorado, USA) (*CHI '17*). Association for Computing Machinery, New York, NY, USA, 1–14. <https://doi.org/10.1145/3025453.3025842>
- [48] Junhan Zhou, Yang Zhang, Gierad Laput, and Chris Harrison. 2016. AuraSense: Enabling Expressive Around-Smartwatch Interactions with Electric Field Sensing. In *Proceedings of the 29th Annual Symposium on User Interface Software and Technology* (Tokyo, Japan) (*UIST '16*). Association for Computing Machinery, New York, NY, USA, 81–86. <https://doi.org/10.1145/2984511.2984568>